Journal of the Physical Society of Japan
Vol. 74, No. 12, December, 2005, pp. 3127–3130

Forward and Backward Drift Motions and Inversion of Drift Directions in Small Lattice Gas System

Akinori AWAZU

Department of Physics, University of Tokyo, 7-3-1 Hongo, Bunkyo-ku, Tokyo 113-0033

(Received July 22, 2005; accepted September 22, 2005)

The drift motions of particles in a nonequilibrium lattice gas system are investigated. We consider a system that consists of two particles interacting repulsively and the potential forces acting on these particles. When only one particle is driven by an external driving field, the other particle shows the following two types of drift motions on the average, depending on the field strength, under certain conditions: I) The particle drifts in the same direction as the external field (forward drift) if the external field is sufficiently strong. II) The particle drifts in the opposite direction to the external field (backward drift) if the external field is of a certain strength. We explain the mechanisms of this phenomenon by considering the transition diagrams.

KEYWORDS: nonequilibrium lattice gas, inversion of drift directions, flagellar motor
DOI: 10.1143/JPSJ.74.3127

Nonequilibrium lattice gases are simple mathematical models which have been useful and important in the studies of the universal properties of nonequilibrium systems with a numerous degrees of freedom.[1] Recently, many varieties of nonequilibrium phenomena such as nonequilibrium phase transitions,[2] a variety of particle flows,[3–7] appearances of long-range spatial correlations,[8,9] the fluctuation theorem,[10] and the mathematical foundations of nonequilibrium statistical mechanics and thermodynamics have been investigated through such lattice gases.[11–13]

In this letter, we investigate the drift motions of particles in a lattice gas system along a circle which consists of only two particles interacting repulsively and the potential forces acting on them. Under nonequilibrium conditions, lattice gas systems have been known to show some nontrivial phenomena, such as the appearance of long-range spatial correlations, even if the system involves only two particles.[9] In our system, the following novel phenomena are found when only one particle is driven by an external driving field; while the driven particle always drifts in the same direction as the external field, the other particle may drift in two directions, the same as or opposite the direction of the external field, depending on the field strength.

In the following sections, the details of numerical and analytical results are shown. First, we introduce our model and show the numerical results, where the above-mentioned drift motions are observed. Next, we explain the mechanism of these phenomena by considering the transition diagrams.

Now, we introduce a lattice gas model, which belongs to a class of driven diffusive two-channel systems.[5] We consider a lattice system with two parallel one-dimensional lanes along a circle where each lane involves L sites with a periodic boundary.[5–7] Each lane contains only one particle which hops randomly to the nearest sites without changing lanes. The sites occupied by particles in the first and second lanes are denoted x_1 and x_2, respectively, which are given as integer numbers from 0 to $L-1$.

The effect of potential forces acting on the particles is described by the following Hamiltonian:

$$H(x_1, x_2) = V(x_1) + V(x_2) + V_{12}(x_1, x_2), \tag{1}$$

where $V(x)$ represents the one-body potential on each lane, and $V_{12}(x_1, x_2)$ represents the interaction potential between the two particles. Furthermore, an external driving field is applied to the particle on the second lane. We denote the field strength F.

The time evolution of this system is described by the iteration of the following three steps. First, one of the two particles is randomly chosen. Let the position of the chosen particle be x. Second, its neighbor site y, $x-1$ or $x+1$, is randomly chosen. Third, the chosen particle moves from x to y with the probability

$$c(x, y; x_1, x_2) = \frac{1}{1 + \exp[Q(x \to y; x_1, x_2)/k_{\mathrm{B}}T]}, \tag{2}$$

with

$$\begin{aligned} &Q(x \to y; x_1, x_2) \\ &\quad = H(x_1', x_2') - H(x_1, x_2) - F(x_2' - x_2), \end{aligned} \tag{3}$$

where $(x_1', x_2') = (x_1, y)$ when $x = x_2$, and $(x_1', x_2') = (y, x_2)$ when $x = x_1$.[14] k_{B} is the Boltzmann constant and T is temperature. Here, the time step is given by [number of above iterations]/[number of particles (= 2)].[15]

Specifically, we study the case where $V(x) = V_b|L/2 - x|$ (Fig. 1), and $V_{12}(x_1, x_2) = d\delta_{x_1, x_2}$ using the $L \times L$ unit matrix δ_{ij}. Also, we focus on the case $L = 4$. We have found that this size is minimum to exhibit the phenomenon we demonstrate in the presented paper.

Now, we demonstrate the simulation of this system. In the following section, we only consider cases with $k_{\mathrm{B}}T \ll d$ and $F > 0$ for simplicity. First, we focus on the dynamical aspects for the case with $V_b \sim d$.

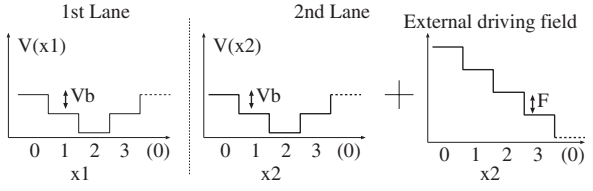

Fig. 1. Illustrations of effects of potential and external field in each lane.

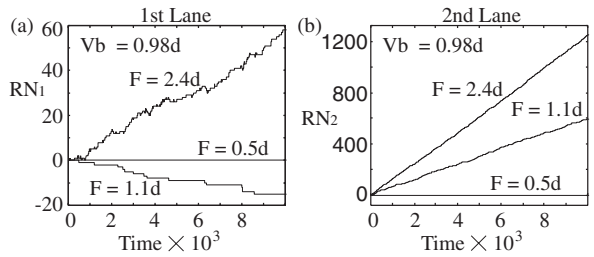

Fig. 2. Typical temporal evolutions of rotation numbers of particle in (a) first lane (RN_1) and (b) second lane (RN_2) for $F = 0.5d$, $1.1d$ and $2.4d$ under $V_b = 0.98d$ and $k_BT = 0.01d$.

Figures 2(a) and 2(b) show typical temporal evolutions of the rotation numbers of the particle in (a) the first lane (RN_1) and (b) the second lane (RN_1) for $F = 0.5d$, $1.1d$ and $2.4d$ under $V_b = 0.98d$ and $k_BT = 0.01d$. Here, RN_i is defined as the number of rotations along the circle by the particle in the ith lane in the direction $x_i : 0 \to 1 \to \cdots \to (L-1) \to 0 \to$. As shown in Fig. 2(b), the drift direction of the particle in the second lane is always the same as the direction of the external field independent of F. On the other hand, as shown in Fig. 2(a), the drift direction of the particle in the first lane changes depending on F; the drift direction of the particle is the same as the direction of the external field for a large F, but it becomes opposite that of the external field following a decrease in F. Here, such former and latter motions of the particle in the first lane are named forward and backward drifts, respectively.

Figures 3(a) and 3(b) show the rotation frequency of the particle in (a) the first lane (RF_1) and (b) the second lane (RF_2) as a function of F/d for several V_b/d ($V_b = 0.4d$, $0.98d$ and $1.6d$) with $k_BT = 0.01d$. Here, the rotation frequency of the particle in the ith lane is defined as $RF_i \equiv (RN_i(\tau) - RN_i(0))/\tau$ with time $\tau \to \infty$. As shown in Fig. 3(b), the drift direction of the particle in the second lane is always the same as the direction of the external field.

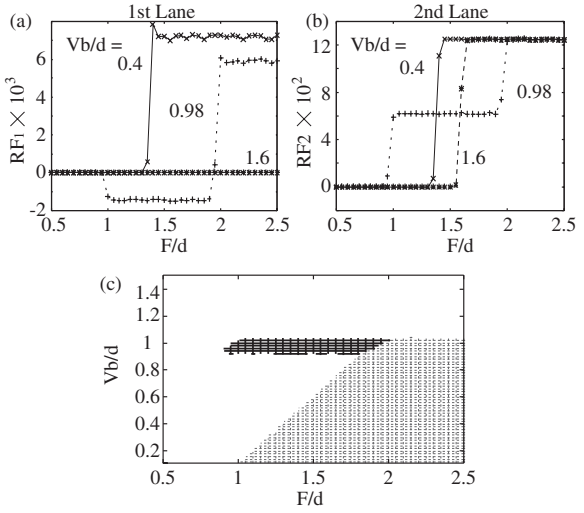

Fig. 3. Rotation frequency of particle in (a) first lane (RF_1) and (b) second lane (RF_2) as a function of F/d for several V_b ($V_b = 0.4d$, $0.98d$ and $1.6d$) with $k_BT = 0.01d$. (c) Phase diagram for drift direction of particle in first lane. The gray area indicates $RF_1 > 0$ and the black area indicates $RF_1 < 0$.

On the other hand, the dynamical properties of the particle in the first lane change depending on the relationship between V_b and d as shown in Fig. 3(a): I) Only forward drift appears when $V_b \ll d$. II) Forward and backward drifts appear depending on F when $V_b \sim d$. III) There are no drift motions independent of F when $V_b \gg d$. Figure 3(c) gives the phase diagram for the drift directions of a particle in the first lane as a function of F and V_b. Here, the gray region indicates $RF_1 > \delta$, and the black region indicates $RF_1 < -\delta$, where $\delta = 10^{-4}$ is set as an example. As shown in this figure, the region where the backward drift appears is given by a certain range of F and V_b space around $F \sim d$ and $V_b \sim d$.

Now, we try to explain the mechanism of our obtained phenomena. First, we name all states of this system using the sites occupied by the particles in each lane (x_1, x_2). Since $L = 4$, this system has 16 states from $(0,0)$ to $(3,3)$. The transitional tendency from (x_1, x_2) to (x_1', x_2') is given by $Q(x \to y; x_1, x_2)$, which was defined previously. Here, $(x_1', x_2') = (x_1, y)$ when $x = x_2$, and $(x_1', x_2') = (y, x_2)$ when $x = x_1$. Then, we obtain the transition diagrams; including all information on the transitions between states.

Figure 4 shows the typical transition diagrams in the cases where (a) $F \sim 0.5d$, (b) $F \sim d$ and (c) $F \sim 2.5d$ under

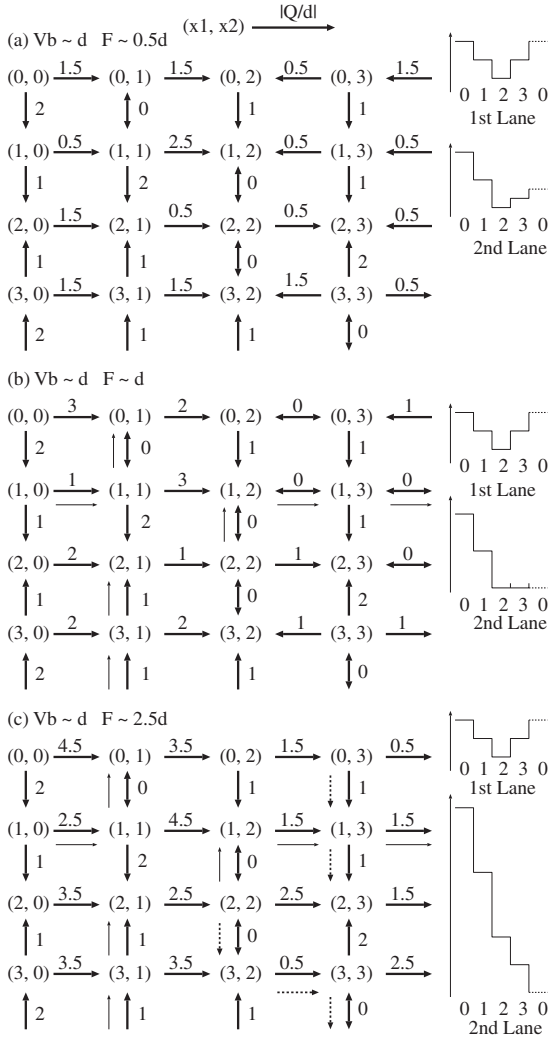

Fig. 4. Typical transition diagram (left) and illustration of effect of potential and external field in each lane (right) for (a) $F \sim 0.5d$, (b) $F \sim d$, (c) $F \sim 2.5d$ with $V_b \sim d$.

$V_b \sim d$. Here, (i, j) indicates the state (x_1, x_2), the arrows give the direction of the transition with a probability higher than ~ 0.5 implying $Q(x \to y; x_1, x_2)/d \lesssim 0$, and the values beside these arrows indicate the value of $|Q(x \to y; x_1, x_2)/d|$. The motion of the system is represented by the random walk caused by the fluctuation with $k_B T$ in the transition diagram. Here, the transition in a vertical direction indicates the motion of the particle in the first lane, and that in a horizontal direction indicates the same in the second lane. For simplicity, we consider the case with low temperature, i.e., $1 \gg k_B T/d > 0$. In this case, only transitions in the directions with $Q(x \to y; x_1, x_2)/d \lesssim 0$ are allowed due to the smallness of $k_B T$.

The appearance of the forward and backward drift motions of the particle in the first lane as shown in Figs. 2 and 3 is explained as follows. Figure 4(a) gives a typical diagram in the cases where $V_b \sim d$ for $F \ll d$. In this diagram, a state $(x_1, x_2) = (2, 3)$ is an attractor. This implies that particles in both lanes drift little, which is consistent with the results in Figs. 2 and 3.

On the other hand, if F increases to $\sim d$, the system can escape from the state $(x_1, x_2) = (2, 3)$ as shown in Fig. 4(b). In such a situation, some transition paths, including the horizontal rotation from left to right, appear in the diagram. This means the particle in the second lane continues to drift in the same direction as that of the external field. Moreover, it is remarkable that this diagram also has the transition paths with the vertical rotation from bottom to top; for example, $(2, 2) \to (1, 2) \to (1, 3) \to (1, 0) \to (1, 1) \to (0, 1) \to (3, 1) \to (2, 1)$ [as indicated by thin arrows in Fig. 4(b)]. However, this diagram has no paths with the vertical rotations from top to bottom. This fact means that, due to the drift of the particle in the second lane, the particle in the first lane drifts in the direction opposite that of the external field.

If F exceeds $\sim 2d$, the direction of the arrow between $(x_1, x_2) = (3, 2)$ and $(x_1, x_2) = (3, 3)$ in the diagram changes. Then, as in Fig. 4(c), the diagram not only has the transition paths with vertical rotations from bottom to top but also those from top to bottom. In this case, the drift direction of the particle in the first lane becomes the same as that of the external field as mentioned below.

In Fig. 4(c), the following two facts were clearly apparent; i) The system tends to stay in the states $(x_1, x_2) = (2, j)$ for most of the time. ii) The state $(x_1, x_2) = (2, 2)$ gives an entrance to the transition paths with both vertical rotations. Then, the paths with vertical rotations starting from $(x_1, x_2) = (2, 2)$ in the diagram contribute predominantly to the motions of the particle in the first lane.

It is noted that the shorter path is generally easier to realize. Thus, we consider the shortest path from $(x_1, x_2) = (2, 2)$ to $(x_1, x_2) = (2, j)$ with the vertical rotation as the main path that gives the motion of the particle in the first lane. The shortest path with the rotation from bottom to top starting from $(2, 2)$ is given by $(2, 2) \to (1, 2) \to (1, 3) \to (1, 0) \to (1, 1) \to (0, 1) \to (3, 1) \to (2, 1)$ [as indicated by thin arrows in Fig. 4(c)]. On the other hand, the shortest path with the rotation from top to bottom is given by $(2, 2) \to (3, 2) \to (3, 3) \to (0, 3) \to (1, 3) \to (2, 3)$, which is shorter than the previous [as indicated by broken arrows in Fig. 4(c)]. Thus, the latter path contributes predominantly to the transitions in a vertical direction in the diagram. This means that the particle in the first lane drifts in the same direction as that of the external field on the average.

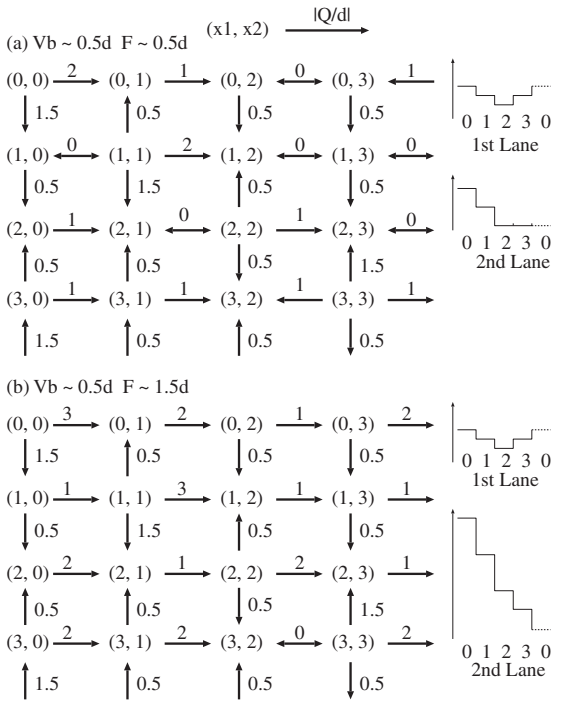

Fig. 5. Typical transition diagram (left) and illustration of effect of potential and external field in each lane (right) for (a) $F \sim 0.5d$, (b) $F \sim 1.5d$ with $V_b \sim 0.5d$.

Thus, in the first lane, forward and backward drift motions appear depending on the strength of the external field.

In cases where $V_b \ll d$, the typical transition diagrams are given as in Fig. 5. In such cases, only the forward drift motion appears as follows. For a small F, the particles in both lanes drift little because an attractor exists at the state $(3, 2)$ as in Fig. 5(a). With the increase in F to $F \sim 1.5d$, the system can escape from the state $(3, 2)$ as in Fig. 5(b). In this case, we naturally found that the vertical rotation from top to bottom tends to be realized in the transition diagram in a similar manner to that in Fig. 4(c). These results are consistent with those in Fig. 3. In a similar way, the mechanisms of the drift motion given in cases where $V_b \gg d$ are also easily explained.

In this letter, we investigated the drift motions of a nonequilibrium small lattice gas system. We found that this system shows two types of drift motion and inversion of the drift direction depending on the strength of the external field by a simple mechanism.

Phenomena similar to our results have been observed, such as the motions of the flagellar motor in bacteria. The flagellar motor is a rotational motor where a rotor realizes steady rotations due to the unique directional flows of protons driven by the electrochemical potential gradient across the membrane.[16–18] Here, it is remarkable that this rotor shows both directional rotations, clockwise and counterclockwise depending on the environment around the cell.

Such motions have been obtained by our system, where the particle in the first lane, that in the second lane and the external field in our model correspond to the rotor, the

proton and the electrochemical potential gradient in the flagellar, respectively. Thus, we expect our results to provide important hints and bases to uncover the possible mechanism for several characteristics of this motor. The detailed studies for this motor, other biological motors or the ion pumps[19] based on the presented study are important issues for the future.

In the presented study, only the behaviors of the system in cases where $L = 4$ and each lane involves only one particle are investigated. Now, we shall investigate more general cases with a larger L, more than three lanes, and multiple particles existing in each lane.

Acknowledgment

The author thanks to M. Sano, S. Ishihara and K. Hayashi for useful discussions. This research was supported in part by a Grant-in-Aid for JSPS Fellows (10039).

1) B. Schimttmann and R. K. P. Zia: *Statistical Mechanics of Driven Diffusive Systems* (Academic Press, London, 1995).
2) S. Katz, L. J. Lebowitz and H. Spohn: J. Stat. Phys. **34** (1984) 497.
3) B. Derrida: Phys. Rep. **301** (1998) 65.
4) S. Takesue, T. Mitsudo and H. Hayakawa: Phys. Rev. E **68** (2003) 015103.
5) V. Popkov and G. M. Schütz: J. Stat. Phys. **112** (2003) 523.
6) A. Awazu: J. Phys. Soc. Jpn. **67** (1998) 1071.
7) T. Mitsudo and H. Hayakawa: to be published in J. Phys. A; cond-mat/0501009.
8) P. Garrido, L. J. Lebowitz, C. Maes and H. Spohn: Phys. Rev. A **42** (1990) 1954.
9) H. Tasaki: cond-mat/0407262.
10) J. Lebowitz and H. Spohn: J. Stat. Phys. **95** (1999) 333.
11) H. Spohn: *Large Scale Dynamics of Interacting Particles* (Springer-Verlag, Berlin, 1991).
12) B. Derrida, J. Lebowitz and E. R. Speer: Phys. Rev. Lett. **89** (2002) 030601.
13) K. Hayashi and S. Sasa: Phys. Rev. E **68** (2003) 035104.
14) $Q(x \to y; x_1, x_2) = H(x_1', x_2') - H(x_1, x_2) - F$ holds when $x = x_2 = L - 1$ and $y = x + 1$, and $Q(x \to y; x_1, x_2) = H(x_1', x_2') - H(x_1, x_2) + F$ holds when $x = x_2 = 0$ and $y = x - 1$.
15) We also obtained qualitatively the same results if we employ the Metropolis rule.
16) B. Alberts, A. Johnson, J. Lewis, M. Raff, K. Roberts and P. Walter: *Molecular Biology of the Cell* (Garland Science, New York, 2002) 4th ed.
17) F. Oosawa and S. Hayashi: J. Phys. Soc. Jpn. **52** (1983) 4019.
18) T. Kubori, N. Shimamoto, S. Yamaguchi, K. Namba and S. Aizawa: J. Mol. Biol. **226** (1992) 433.
19) E. Muneyuki and T. A. Fukami: Biophys. J. **78** (2000) 1166.